



## Trends in heat and cold wave risks for the Italian Trentino Alto-Adige region from 1980 to 2018

Martin Morlot<sup>1</sup>, Simone Russo<sup>2</sup>, Luc Feyen<sup>2</sup>, and Giuseppe Formetta<sup>1</sup>

<sup>1</sup> University of Trento, Department of civil, environmental, and mechanical engineering,  
via Mesiano, 77, 38123, Trento (Italy)

<sup>2</sup> European Commission, Joint Research Centre

Corresponding author: Giuseppe Formetta, [Giuseppe.formetta@unitn.it](mailto:Giuseppe.formetta@unitn.it)

### Abstract

Heat waves (HW) and cold waves (CW) can have considerable impact on people.

Mapping risks of extreme temperature at local scale accounting for the interactions between hazard, exposure and vulnerability remains a challenging task. In this study, we quantify human risks from HW and CW at high resolution for the Trentino-Alto Adige region of Italy from 1980 to 2018. We use the Heat Wave Magnitude Index daily (HWMId) and a Cold Wave Magnitude Index daily (CWMId) as temperature-based indicators and apply a Tweedie zero-inflated distribution to derive hazard intensities and frequencies. The hazard maps are combined with high-resolution maps of population, for which the vulnerability is quantified at community and city level using a set of eight socioeconomic indicators. We find a statistically significant increase in HW hazard and exposure, with 6.0-times more people exposed to extreme heat after 2000 compared to the last two decades of the previous century. CW hazard and exposure remained stagnant over the studied period in the region. We observe a general trend towards increased resilience to extreme temperature spells over the region. In the larger cities of



the region, however, we find that vulnerability has increased due to an ageing population and more single households. HW risk has risen practically everywhere in the region, indicating that the reduction in vulnerability in the smaller communities is outpaced by the increase in HW hazard. In the large cities, HW risk levels in the 2010s are 50% larger compared to the 1980s due to the rise in both hazard and vulnerability. Whereas in smaller communities, stagnant CW hazard and declining vulnerability results in reduced CW risk levels, the risk level in cities grew by 20% due to the increased vulnerability over the study period. The findings of our study are highly relevant for steering investments in local risk mitigation measures, while the method can be applied to other regions that have detailed information on hazard, exposure and vulnerability indicators.

## 1 Introduction

Heat waves (HW) and cold waves (CW) are hazards that affect public health and the environment (Gasparrini et al., 2015; Habeeb et al., 2015). With global warming, heat and cold wave intensities and durations are expected to change (Perkins-Kirkpatrick and Gibson, 2017; Russo et al., 2015; Smid et al., 2019), which could increase the risks to society. A recent report showed that in 2018, worldwide 157 million more people were exposed to HW compared to 2000 (Watts et al., 2018). In Europe, on average 55% of the area of Europe was impacted by HW over the last two decades (i.e. with HW events in 2003, 2010, 2015, 2018), accounting for GDP losses of 0.3-0.5% when compared to 0.2% for 1980-2010 (García-León et al., 2021). With regards to CW in Europe, recent winters have claimed lives in Europe with 790 deaths in 2006 and 549 deaths in 2012



(Kron et al., 2019). In Italy, HW have had a strong impact on mortality in the past. In 2003, a 27% mortality increase was reported over August and a 6% increase during the summer compared to the 5 previous years (Michelozzi et al., 2005), while in 2015 there was a 23% increase in July compared to the 5 previous years (Michelozzi et al., 2016).

50 In the Trentino Alto-Adige region (the study region), Conti et al. (2005) showed that for the large heat wave of 2003, mortality increased by 32% in Trento and 28% in Bolzano (the two main cities of the region) compared with the previous year. For Bolzano, Papathoma-Köhle et al. (2014) found that higher hospital admissions in the city occurred during the 2003 HW when comparing it to other years (2006, 2009), particularly among  
55 elderly women. The increase in mortality and among the elderly is also found in Italy for the case of CW, this was the case during the CW of 2012 (de'Donato et al., 2013), with notably an increase in mortality of 47% for the timeframe of the cold spell in the city of Bolzano.

The United Nations Office for Disaster Risk Reduction (UNDRR, 2021) and the  
60 Intergovernmental Panel on Climate change (IPCC, 2014) define risk as a function of hazard, exposure, and vulnerability. Exposure is defined as people, infrastructure, housing, production, and other tangible human assets present in hazard-prone areas. Vulnerability is defined as the conditions that define the susceptibility of an individual, infrastructure or a community to be impacted by the hazard. To successfully quantify  
65 risk, one must be able to measure all three components: hazard, exposure and vulnerability.

Several temperature hazard-exposure studies have been conducted at global (e.g. Chambers, 2020; Dosio et al., 2018), continental (eg. King et al., 2018), or city scale



(e.g. Smid et al., 2019). Most studies focus on human exposure (eg. Chambers, 2020;  
 70 Tuholske et al., 2021), but also the exposure of land area (e.g., Ceccherini et al., 2017;  
 Oldenborgh et al., 2019; Russo et al., 2016). Most of these studies have found  
 increasing trends in exposure to HW and for the studies that also analyzed CW, found  
 decreasing trends for them.

Typically, these previous studies on the topic, have however relied on using qualitative  
 75 numerical thresholds to define the severity of the events and define exposure according  
 these thresholds. However, HW and CW hazards can also be defined by their return  
 period but fitting extreme value distributions to define these is difficult due to the  
 absence of events (zero values) for multiple years in their time series; Generalised  
 extreme value distribution (GEV) and non-stationary-techniques (Dosio et al., 2018;  
 80 Kishore et al., 2022; Russo et al., 2019) have enabled to estimate HW and CW's return  
 periods, but both approaches circumvent this absence rather than considering the zero  
 values directly. We therefore use for the first time the zero-inflated distribution form of  
 Tweedie (Jorgensen, 1987; Tweedie, 1984) to estimate HW and CW frequency of  
 occurrence, which enables for the direct fitting of zero values. The Tweedie distribution  
 85 has been used mostly for the purpose of insurance claims analysis, but has also seldom  
 been applied in the field of natural hazards, such as a zero-inflated Poisson distribution  
 to model heat wave mortality (Kim et al., 2017), to analyze droughts (Tijdeman et al.,  
 2020), or for rainfall analysis (Dunn, 2004; Hasan and Dunn, 2011).

To perform a risk analysis, one must know the vulnerability to the hazard. To this end,  
 90 the vulnerabilities to temperature extremes are complex to quantify. Recent studies  
 have developed temperature-mortality relationships (e.g., Gasparrini et al., 2015) at the



scale of cities. However, this requires that the city has substantial population, and sufficiently long records of mortality and temperature. HW and CW vulnerability can also be approximated by combination of several socioeconomic indicators. At the community  
95 level in the United States, factors such as social isolation, presence of air conditioning, proportion of elderly and proportion of diabetics in the population were found to be key for human vulnerability to temperature extremes (Reid et al., 2009). In Korea at the county level, Kim et al. (2017) found that elderly living alone, agricultural workers and unemployed affect vulnerability to heat wave days and tropical nights. Temperature  
100 vulnerability has also been appraised at city scale for HW mortality (Ellena et al., 2020) and at regional scale (López-Bueno et al., 2021) for CW mortality. Karanja & Kiage (2021) and Cheng et al. (2021) provide an overview of the different types of indicators used in the literature to characterize vulnerability. The indicators can be diverse, ranging from population structure (e.g. age and health characteristics), social status, economic  
105 conditions, community (cultural) group characteristics, and household physical characteristics. Work on social vulnerability in Italy has used a diversity of indicators found in the census records (Frigerio and De Amicis, 2016). Other analyses conducted for Italian cities focused on neighborhood and building levels to produce HW vulnerabilities for Milano (Bhattacharjee et al., 2019), and HW vulnerability and risks for  
110 Padua (Maragno et al., 2020).

The risks of HW and CW are often assessed using different methodologies depending on the objectives of the study. On a global scale, Russo et al (2019), establish a risk index using the probabilities of HW as hazard, where the exposure is the normalized population and vulnerability is based on a socio-economic indicator (human



115 development index). For Italy, Morabito et al (2015) conducted a risk analysis of heat on  
elderly in the major cities, using the elderly population as the only vulnerability factor  
and summer average temperatures for the period 2000-2013 to quantify the hazards.

The Trentino Alto-Adige region of Italy is composed of two provinces (Trento and  
Bolzano). It is a region of interest to study HW and CW risks due to an expected  
120 increase in the number and percentage of elderly people (Papathoma-Köhle et al.,  
2014), which in combination with increasing temperature extremes in view of climate  
change could increase human risks. Few studies have attempted to quantify HW and  
CW impacts for the cities in the region (e.g. Trento and Bolzano), such as Conti et al.  
(2005) as part of their studies on Italian cities and Papathoma-Köhle et al. (2014) who  
125 studied impacts in Bolzano. The findings of these study are limited for two reasons: they  
use few samples per day (Papathoma-Köhle et al., 2014) and short timeframes, e.g.,  
comparing only 2002 to 2003 in Conti et al. (2005) and considering only 4 years of data  
in Papathoma-Köhle et al. (2014). However, conducting spatial-temporal risks analyses  
of HW and CW are typically not done over a large timeframe at such a detailed location  
130 scale (city-level); yet these are important to forge a better understanding of the  
spatiotemporal human risks and their underlying drivers which are critical to plan risk-  
mitigation measures at the local level.

The aim of this article is to solve some of these previous limitations while quantifying  
heat and cold waves hazards, the human exposure, vulnerability, and risk for the at the  
135 high-definition city scale for the Trentino-Alto-Adige region over the period 1980-2018.  
The quantification of the hazard and its return period will be performed using the  
Heatwave magnitude index HWMId and its cold wave counterpart CWMId (Russo et al.,



2014, 2015) and using the novel method of fitting the Tweedie distribution to help us estimate the exposure and risk.

## 140    **2    Study Area**

The Trentino Alto-Adige region (

Figure 1: The Trentino Alto-Adige region) is a mountainous region in northern Italy, which borders Austria. The elevation of the region varies from 65m for lake Garda to 3,439m for Lagaunspitze. It is composed of two provinces (Province of Trento and  
145    Province of Bolzano). Its most populous cities are the two provincial capitals -- Trento and Bolzano -- as well as minor cities Merano and Rovereto (both have a population of over 30000). The main rivers in the region are the Adige, and its tributary, the Isarco. Due to its diverse geography, the climate is also diverse ranging from Subcontinental to Alpine on the Koppen classification (Fратиanni and Acquaotta, 2017).

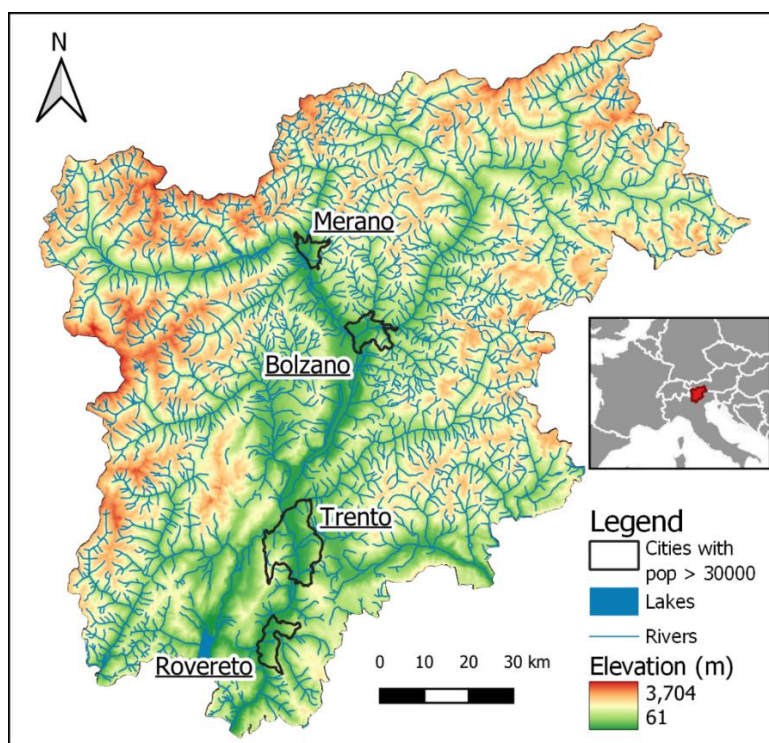


Figure 1: The Trentino Alto-Adige region

### 3 Methodology

#### 3.1 Temperature data

In order to quantify the HW and CW hazard, we used the freely available spatial  
 temporal temperature dataset by Crespi et al. (2021). It consists of gridded daily  
 temperatures for the entire Trentino Alto-Adige region covering the period of 1980-2018  
 at a resolution of 250 meters. The dataset is obtained with the anomaly-based approach  
 taking into account elevation of the local station observations; the dataset has  
 undergone a quality analysis and control against the stations' observations (Crespi et al.  
 2021).





### 3.2 Hazard quantification, fitting and sizing

To quantify the hazard, we used HWMId (Russo et al., 2015) and CWMId (Smid et al., 2019).

For HWMId, from the temperature time series in each grid cell, we select the days

165 where the temperature is above the 90<sup>th</sup> percentile of the dataset  $A_d$  (Equation 1):

$$A_d = \bigcup_{y=1981}^{2010} \bigcup_{i=d-15}^{d+15} T_{y,i} \quad (1)$$

where  $y$  corresponds to the year,  $i$  to the day, and  $T_{y,i}$  correspond to the temperature of the corresponding year and day and the dataset  $A_d$  corresponds to the temperature

170 data for 30 years, centered on a 31-day window for the day in question. Three consecutive days above this threshold correspond to a HW.

Then the magnitude of the HW is calculated by Equation 2:

$$HM_d(T_d) = \begin{cases} \frac{T_d - T_{30y25p}}{T_{30y75p} - T_{30y25p}} & \text{if } T_d > T_{30y25p} \\ 0 & \text{if } T_d \leq T_{30y25p} \end{cases} \quad (2)$$

175 where  $HM_d(T_d)$  corresponds to the heat daily magnitude,  $T_d$  the temperature of the day in question and  $T_{30y25p}$  and  $T_{30y75p}$  correspond to the 25<sup>th</sup> and 75<sup>th</sup> percentile temperature for the 30 years used as a reference. The highest cumulative magnitude is retained for each year and only consecutive days above 0 are considered when calculating it.



For CWMId, CW are defined as three consecutive days with daily temperatures below  
 180 the 10<sup>th</sup> percentile of  $A_d$ . The magnitude is then redefined to adapt to low temperatures  
 as in equation 3:

$$CM_d(T_d) = \begin{cases} \frac{T_d - T_{30y75p}}{T_{30y75p} - T_{30y25p}} & \text{if } T_d < T_{30y75p} \\ 0 & \text{if } T_d > T_{30y75p} \end{cases} \quad (3)$$

where  $CM_d(T_d)$  corresponds to the cold daily magnitude,  $T_d$  the temperature of the day  
 185 in question and  $T_{30y25p}$  and  $T_{30y75p}$  correspond to the 25<sup>th</sup> and 75<sup>th</sup> percentile temperature  
 for the 30years used as a reference. Similarly, the lowest cumulative magnitude is  
 retained for each year and only consecutive days below 0 are considered when  
 calculating it.

For both the values of HWMId and CWMId to be positive and on the same interval, the  
 190 absolute values of CWMId are retained from this point on.

The values can then be modelled with a specific probability distribution to estimate the  
 return periods of HW and CW. Considering that HWMId and CWMId are both defined in  
 $[0, +\infty[$ , we use the Tweedie distribution (Jorgensen, 1987; Tweedie, 1984), a  
 distribution that can act as zero-inflated, thus accounting for the presence of zeros  
 195 directly. The Tweedie distribution is an exponential dispersion model which has a  
 probability density function of the form (equation 4):

$$f(y, \theta, \Phi) = a(y, \Phi) * \exp \left[ \frac{1}{\Phi} \{y\theta - \kappa(\theta)\} \right] \quad (4)$$



where  $\Phi$  corresponds to its dispersion parameter that is positive,  $\theta$  to its canonical  
 200 parameter, and  $\kappa(\theta)$  the cumulant function. The function  $a(y, \Phi)$  generally cannot be  
 written in closed form. The cumulant function is related to the mean ( $\mu_y = \kappa'(\theta)$ ) and  
 variance ( $\sigma_y = \Phi * \kappa''(\theta)$ ) and in the case of a Tweedie distribution the variance has a  
 power relationship with the mean (Equation 5):

$$\sigma_y = \Phi * (\mu_y)^p$$

205 (5)

where  $p$  corresponds to the power parameter that is positive.

Depending on the value of  $p$ , the distribution will behave differently. In the case where  $p$   
 is between 1 and 2, it belongs to the compound Poisson-gamma distribution with a  
 mass at zero, while other  $p$  values can make the distribution correspond to a normal,  
 210 Poisson, or gamma distribution, among others. The use of the Tweedie distribution is  
 retained as it permits to consider the zero values, while also considering other  
 distributions should there be an absence of zero values.

We fit the distribution to the previously found HWMId and CWMIId values with the help  
 of the Tweedie R package (Dunn, 2021). An example of the fitted distribution for  
 215 Bolzano and Trento can be found in the supplementary material (Figure S – 1). It is also  
 possible to use the same package to estimate a quantile using the fitted distribution.  
 This enables to estimate specific return levels for return periods  $T$  for both HWMId and  
 CWMIId. For this study two return levels are retained, 5 years (HW5Y for HW, and  
 CW5Y for CW) and 10 years (HW10Y for HW and CW10Y for CW).



220 For statistical fit verification, the Kolmogorov–Smirnov (KS) test on two samples is used  
with one sample being the found HWMId or CWMId values, and the other sample being  
a randomly generated sample using the fitted distribution value. This goodness of fit of  
test is one of the most commonly used in the literature for the case of the corresponding  
zero inflated Tweedie distribution (Goffard et al., 2019; Johnson et al., 2015; Rahma  
225 and Kokonendji, 2021). The null hypothesis of this test is that the two sample belong to  
the same distribution. If the P-value for this test is below the significance level  $\alpha$  of 5%,  
the null hypothesis is rejected, otherwise we cannot reject the null hypothesis at this  
significance level.

### 3.3 Exposure quantification

230 To quantify the population exposed to HW and CW we use time-varying population  
from the Global Human Settlement Layer (GHSL) (Schiavina et al., 2019). The data is  
available at a resolution of 250m for the following years: 1975, 1990, 2000 and 2015.  
Both this data, and the population count done by the Italian national statistical institute,  
indicate a growing population throughout the region (overall 23%). Following recent  
235 studies (King and Harrington, 2018; Russo et al., 2019), for each year of the time period  
a pixel is considered exposed if the HW/CW hazard (measured by HWMId or CWMId) is  
greater than zero or a specified return level value. For that year, the population exposed  
in the region is the sum of all exposed pixels in the region. The percentage of population  
exposed is obtained dividing the population exposed by the total population in the  
240 region at that time. The results for the percentage of population exposed are calculated  
on annual basis over the study period (1980-2018).



### 3.4 Vulnerability quantification

We express HW and CW vulnerability using eight indicators as in Ho et al. (2018), who quantify community vulnerability to HW and CW events based on extreme age, household physical characteristics, social status and economic conditions. The list of variables considered are reported in Table 1.



*Table 1: Vulnerability indicators used (after Ho et al., 2018)*

Category	Indicator	Definition
Extreme Age	Older Age	Population over 55 years old
	Infants	Population under 5 years old
Household physical characteristics	People in old houses	Number of household living in housing built prior to 1960
	People in poor living condition	Population living in at risk housing
Social Status	Low education population	Population with low education (no diploma or degree)
	People living alone	Number of single-person households
Economic Status	Low-income population	Population with low income
	Unemployed	Unemployment rate

250 The spatially varied indicators are freely available in the census records (i.e. sub-city level) from the Italian national statistical institute (Istat.it - 15° Censimento della popolazione e delle abitazioni 2011, 2021) for three different years (1991, 2001 2011). Given the data time constraints, vulnerability is thus derived for those years only.

The methodology to quantify vulnerability uses the equal weight analysis (EWA) with the  
 255 indicators being standardized between 0 and 1 prior to aggregation according to Liu et al, (2020).



### 3.5 Risk Quantification

Risk here is assumed to be a function of hazard, exposure and vulnerability, which are multiplied to quantify risk (UNDRR, 2021). This is one of the two most commonly used approaches in literature (Dong et al., 2020; Quader et al., 2017; Russo et al., 2019), with the other approach being the addition of the different risk components.

Multiplication when compared to addition is found to better highlight the complex relationship between the different components, as the multiplication of the multivariate probabilities of independent variables follow a product law (El-Zein and Tonmoy, 2015; Estoque et al., 2020; Peng et al., 2017).

The risk is calculated as per Dong et al. (2020) (equation 6):

$$\text{Risk} = \sqrt[3]{\text{Hazard} * \text{Exposure} * \text{Vulnerability}} \quad (6)$$

with each of the risk components having a value in [0,1]. Hazard is the probability of HWMIId/CWMIId derived from the Tweedie distribution. Exposure is the standardized population density. The vulnerability derived from standardized variables is also between [0,1]. The resulting risk is therefore also bound by 0 and 1, with 0 corresponding to the lowest level of risk and 1 to the highest level of risk.

On a temporal scale, the yearly risk calculation is done using the closest records of vulnerability and exposure to the year in question. This means, that for the 2003 HW risk, the 2003 HW hazard probabilities are combined with 2001 vulnerabilities (the closest census available year) and 2000 population (the closest population map



available). The risk is calculated at city level because vulnerability is not available at a higher resolution.

#### 280 4 Results and discussions

For HW hazard intensities, the most notable year on record (1980-2018) in the region is 2003, where HWMId reached a pixel maximum of 30.4 and a median value of 16.9 over the area (Figure S – 2 in the supplementary material). The second most intense HW occurred in 2015 and the third most intense in 1983. This aligns well with Russo et al. (2015), who have found very high HW in 1983, 2003 and 2015 in their analysis of the ten greatest HW in Europe since 1950. From the six years with the highest median HWMId between 1980 and 2018, four occurred in the last decade (2010, 2013, 2015, 2017), suggesting that climate change is already increasing the frequency of heat waves in the Trentino Alto-Adige region. For CW, only 1985 stands out, with a maximum and median CWMId of 27 and 14.5, respectively, or nearly three times more than that of any other year on record. The second strongest cold wave occurred in 2012. This is in agreement with Jarzyna & Krzyżewska, (2021), who have found cold spells in those years (1985 and 2012) using different methodologies for other locations throughout Europe.

295 A KS test (Figure S – 3 in the supplementary material) shows that the Tweedie distribution provides a good fit for both CWMId and HWMId, with power parameter values between [1,2] for the entire region. The KS goodness of fit test reveals no rejection at a significance level of 5% for any pixel in the region. This permits us to estimate return levels for both HW and CW and analyze trends based on them. The



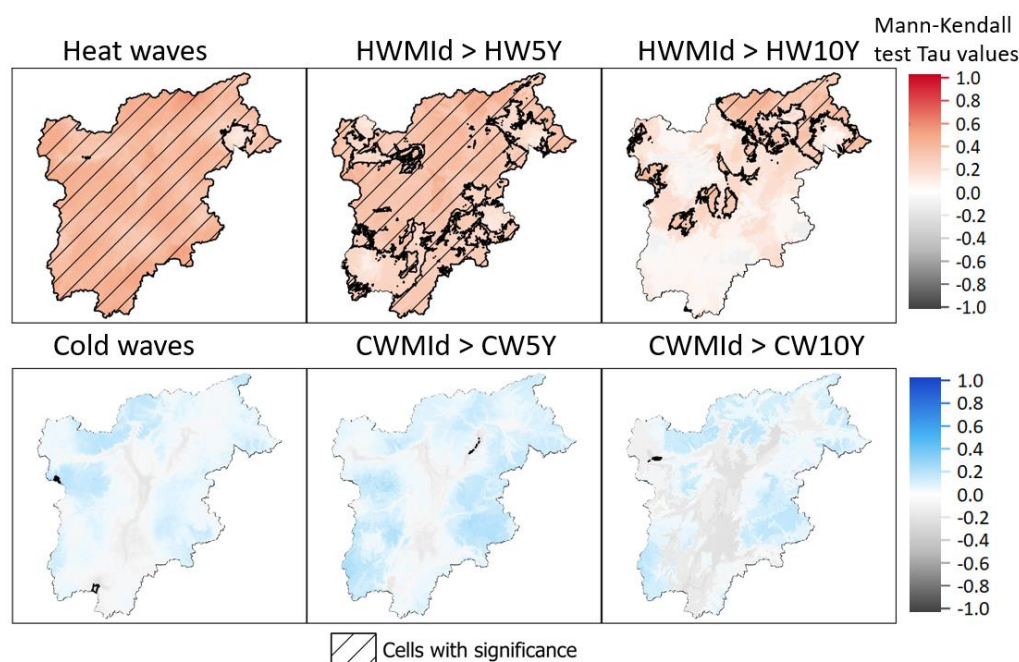


300 return levels for return periods  $T=5$  years (HW5Y, CW5Y) and  $T=10$  years (HW10Y, CW10Y) for every pixel are shown in Figure S – 4 in the supplementary material.

Using a Mann-Kendall trend test (Kendall, 1948), statistically significant positive trends are found for HW in most pixels of the region (Figure 2). HW with a magnitude larger than the 5-year event ( $HW_{MId} > HW5Y$ ) also show a significant increasing trend over a  
305 large part of the region. For rarer events; those larger than the 10-year event ( $HW_{MId} > HW10Y$ ), we find a statistically significant increase in HW intensity only in a portion of the region, mostly in upstream areas in the north but also around Bolzano. In the three previous cases, for the rest of the region, the absence of statistical significance does not permit us to draw conclusions with regards to the trends. For CWs, we do not find  
310 statistically significant trends in any part of the region. The locations of presence / absence of these significant trends are further evidenced using the robust linear model



((Huber, 2011)) and previously used for HW by (Kishore et al., 2022)), see Figure S – 5 in the supplementary material.



315 *Figure 2: Trends in heat waves (HW) and cold waves (CW) using Mann-Kendall's test based on yearly HWMId and CWMId magnitudes from 1980 to 2018*

The significant increasing trend for HW that we find are consistent with literature that reported increasing HW trends in Europe over the last decades (Perkins-Kirkpatrick and  
 320 Lewis, 2020; Piticar et al., 2018; Serrano-Notivoli et al., 2022; Spinoni et al., 2015; Zhang et al., 2020). The lack of trend in CW is also in agreement with previous research that could not detect any trend in extreme cold spells (Jarzyna and Krzyżewska, 2021; Piticar et al., 2018).



In total, between 1980 and 2000, in the study region, about 900 000 people were  
325 exposed to a 5-year HW, 250 000 to 10 HW year heatwave, 3million to 5-year CW and  
1.9 million to 10-year CW. Between 2000 and 2018, the values increased to over  
5millions for 5-year HW and to about 2.5million for 10-year HW but decreased to 2.4  
million for 5-year CW and to 500 000 for 10-year CW. However, due to the importance  
330 to study the percent of population impacted by these different events to understand  
whether these changes are due to demographic changes or the frequency of events.

Figure 3 presents the share of the population exposed to HW and CW intensities larger  
than those of 5-year and 10-year events over the period 1980 to 2018 on a yearly basis.  
It shows that a higher share of the population was exposed to HW more frequently after  
335 2000 compared to the first two decades (80s and 90s). For both return periods, the  
Mann-Kendall test shows a significant increase in population exposed to HW over the  
region (Table T - 1 in the supplementary material). We did not find a trend in human  
exposure to CW in the region. Other statistical tests (Sen's slope and linear model)  
confirm these trends.

340

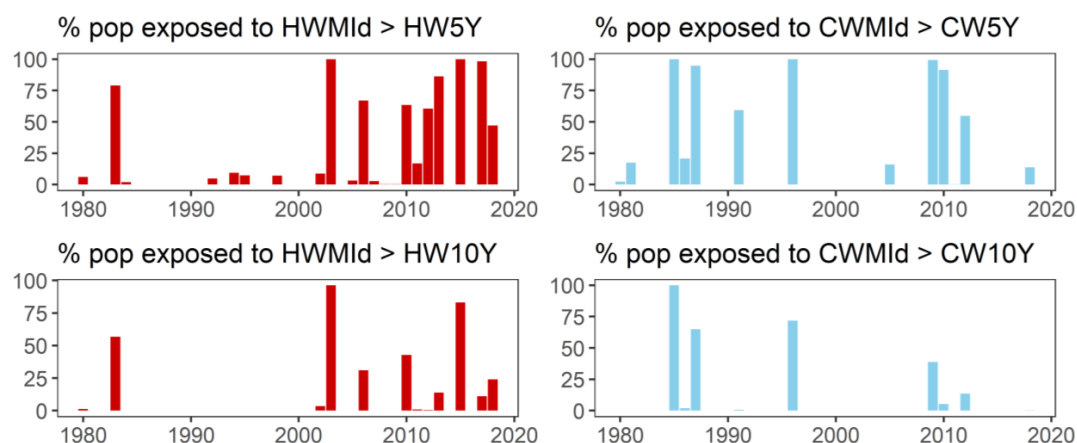


*Figure 3: Percentage of population exposed to heat wave and cold wave events*

The vulnerability for the region (Figure 4) decreases in time, with an average value of 0.42 in 1991, 0.32 in 2001 and 0.27 in 2011. The main reason for the decrease in vulnerability at regional scale is the improvement in overall education level and housing conditions (i.e., fewer people living in old and poor housing conditions). However, by contrast, for the larger cities (those with a population over 30,000: Merano, Bolzano, Trento, Rovereto), the vulnerability has increased from 0.28 in 1991 to 0.30 in 2001 and 0.32 in 2011, averaged for those cities. The increase in these cities' vulnerability relates to the extreme age indicator and social status, with a growing portion of the population above 55 and an increase in the number of isolated households (i.e., people living alone). These two factors (elderly population and isolation) have also been found as some of the main factors for vulnerabilities in other regions of Europe (López-Bueno et al., 2021; Poumadère et al., 2005).

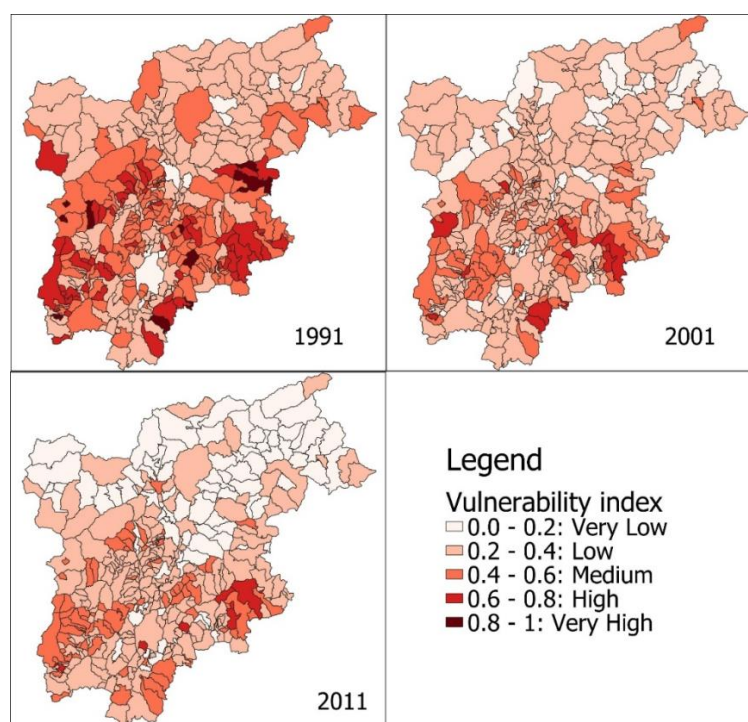


*Figure 4: Calculated vulnerability index for the three years of the census records (1991, 2001, 2011)*

360 The results of our vulnerability analysis somehow contrast with the findings of Frigerio &  
 De Amicis (2016), who report increasing vulnerabilities for municipalities of the Bolzano  
 province and slightly decreasing to steady vulnerabilities in the Trento province. This  
 likely relates to the use of different indicators (employment, social-economic status,  
 family structures, race/ethnicity, and population growth) and a different methodology for  
 365 calculating the vulnerability. Notably in Frigerio & De Amicis (2016) the normalization of  
 indicators is applied across all of Italy as opposed to only over the Trentino Alto-Adige  
 region in this study, which may better characterize local vulnerability.

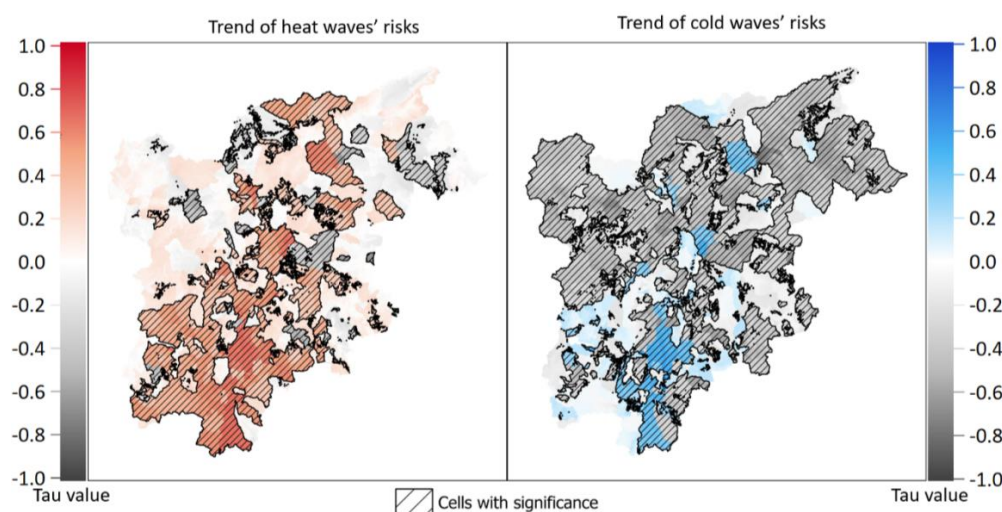


Figure 5 shows the trend in risk for the whole region over the period 1980-2018. The Mann-Kendall test shows a significant increasing trend in HW risk in most of the area, with a decreasing significant risk in some isolated parts of the region of study. While the risk from CW has decreased over most of the region since the 1980s, in the major cities (Trento, Rovereto, Bolzano and Merano), we found an increase in CW risk. The locations of presence/absence of these significant trends are further evidenced using the robust linear model (see Figure S – 6 in the supplementary material).

Decadal means of the annual regional risk values confirm these trends, with the HW risk increasing from 0.113 in the 1980s to 0.126 for the 2010s, while CW risk has decreased from 0.126 in the 1980s to 0.117 in the 2010s. Decadal means of HW risk for the large cities show a stronger trend, with the large-city average risk value increasing from 0.263 to 0.386, or nearly a 50% increase in risk value compared to a 12% increase in HW risk for the whole region. Decadal means of CW risk for the big cities increased from 0.300 in the 1980s to 0.359 in the 2010s, or a 20% increase in CW risk compared to a reduction of 7% for the whole region. Similar findings are found with regards to the increase in HW risks by (Smid et al., 2019)), indicating an increase in the future for European capitals; however the same study highlights a future decrease in CW risk for these same cities. This is in contrast with the main cities of our study, where yet in the last four decades, CW risks are still found to be increasing. This could perhaps also be the case for other cities in mountainous regions such as highlighted by the case of Madrid in (López-Bueno et al., 2021) where its urban area was found to be the most at risk of CW as opposed to its rural area.



390 It is further noted that the highest annual risk levels for both HW and CW coincide with  
 the years with the highest hazard intensity (2003 for HW and 1985 for CW, see Figure S  
 – 7 in the supplementary material), indicating that the hazard is the triggering factor for  
 risk. However, risks are further modulated by exposure and vulnerability. The risks are  
 found to be the highest in the largest cities (Bolzano, Merano, Rovereto and Trento).  
 395 This can be explained in part by the high population density in those cities, which is  
 significantly larger than elsewhere in the region. Another factor is the increasing  
 vulnerabilities in these cities relating to an increase in elderly and single households as  
 previously mentioned.



400 *Figure 5: Trends of heat waves and cold waves risks via the Mann-Kendall test.*





## 5 Summary and conclusions

Our study is one of the first to calculate risks of HW and CW and their trends at the community and city level for a region over 39 years. This is done by first mapping the historical hazard of extreme temperature events using the HWMId and CWMId indicators, we mapped at high resolution (250 m) in the Trentino Alto-Adige region for the period 1980-2018. The hazards are then sized using the novel method of fitting a Tweedie distribution to the HWMId and CWMId values while accounting directly for zero values in their values time series. Exposure is be found using the different fitted hazard levels. Vulnerability is calculated using 8 different socioeconomic indicators. Using all these findings, the spatio-temporal HW / CW risk over the time period and at the city level is calculated.

Over the past 4 decades, HW have occurred more frequently and have become more intense, resulting in an increasing exposure of people to extreme heat spells. For CW, we did not find a trend in hazard frequency and intensity and a fairly constant exposure to extreme cold. In general, vulnerability is decreasing over time in the Trentino Alto-Adige region. However, in the larger cities of the region, vulnerability is increasing due to an ageing population and more single households. It should be noted that the socioeconomic indicators of vulnerability are only available for three points in time, which does not allow to do a proper trend analysis of vulnerability. With regards to risk, for smaller communities in the region in general, a steady but limited increase (+ ~10%) in HW risk and a decrease (- ~9%) in CW risk are found. However, in the larger cities of the region, a much stronger rise in HW risk (+~50%) and an increase of around 20% in CW risk occur. This is linked with demographic changes and the social status of city





425 dwellers, with more people and an ageing population living in cities and an increase in  
the number of people living alone.

The findings of this work shows that municipalities and cities in the Trentino Alto-Adige  
region, but likely also in many other regions, will be exposed especially to more frequent  
and intense heat, while potentially still experiencing the same levels of cold wave  
430 hazard. Our detailed analysis shows where to prioritize risk mitigation measures to  
reduce the hazard and vulnerability. Measures to mitigate heat in cities include, for  
example, greening of cities (Alsaad et al., 2022; Taleghani et al., 2019) , while  
vulnerability could be decreased by improving the social and living conditions of  
citizens, especially of the elderly who are more vulnerable (Orlando et al., 2021;  
435 Poumadère et al., 2005; Vu et al., 2019), particularly in the cities of this region where  
they are becoming more numerous. If detailed data are available for temperature,  
exposure and vulnerability indicators, the methodology presented here could be applied  
to other regions in- and outside Italy to help steer local climate adaptation investments  
at the city level.

440

### **Code availability**

The code used for calculating HWMId and CWMId is free and open source, it is the  
extRemes package of R which is findable here: [https://cran.r-](https://cran.r-project.org/package=extRemes)  
[project.org/package=extRemes](https://cran.r-project.org/package=extRemes).



445 **Data availability**

All data used in this study is available freely and openly online. The temperature

data(Crespi et al., 2021) is available at the following location:

<https://doi.pangaea.de/10.1594/PANGAEA.924502>. The population data from the GHSL

is available at this location: <https://data.jrc.ec.europa.eu/collection/ghsl>. The indicator

450 data used to calculate the vulnerable is available from ISTAT: <https://www.istat.it/en/>.



## 455 References

- Alsaad, H., Hartmann, M., Hilbel, R., and Voelker, C.: The potential of facade greening in mitigating the effects of heatwaves in Central European cities, *Build. Environ.*, 216, 109021, <https://doi.org/10.1016/j.buildenv.2022.109021>, 2022.
- 460 Battacharjee, S., Gerasimova, E., Imbert, C., Tencar, J., and Rotondo, F.: Assessment of Different Methodologies for Mapping Urban Heat Vulnerability for Milan, Italy, *IOP Conf. Ser. Earth Environ. Sci.*, 290, 012162, <https://doi.org/10.1088/1755-1315/290/1/012162>, 2019.
- Ceccherini, G., Russo, S., Ameztoy, I., Marchese, A. F., and Carmona-Moreno, C.: Heat waves in Africa 1981&ndash;2015, observations and reanalysis, *Nat. Hazards Earth Syst. Sci.*, 17, 115–125, <https://doi.org/10.5194/nhess-17-115-2017>, 2017.
- 465 Chambers, J.: Global and cross-country analysis of exposure of vulnerable populations to heatwaves from 1980 to 2018, *Clim. Change*, 163, 539–558, <https://doi.org/10.1007/s10584-020-02884-2>, 2020.
- Cheng, W., Li, D., Liu, Z., and Brown, R. D.: Approaches for identifying heat-vulnerable populations and locations: A systematic review, *Sci. Total Environ.*, 799, 149417, <https://doi.org/10.1016/j.scitotenv.2021.149417>, 2021.
- 470 Conti, S., Meli, P., Minelli, G., Solimini, R., Toccaceli, V., Vichi, M., Beltrano, C., and Perini, L.: Epidemiologic study of mortality during the Summer 2003 heat wave in Italy, *Environ. Res.*, 98, 390–399, <https://doi.org/10.1016/j.envres.2004.10.009>, 2005.
- 475 Crespi, A., Matiu, M., Bertoldi, G., Petitta, M., and Zebisch, M.: A high-resolution gridded dataset of daily temperature and precipitation records (1980&ndash;2018) for Trentino &ndash; South Tyrol (north-eastern Italian Alps), *Earth Syst. Sci. Data Discuss.*, 1–27, <https://doi.org/10.5194/essd-2020-346>, 2021.
- 480 de'Donato, F. K., Leone, M., Noce, D., Davoli, M., and Michelozzi, P.: The Impact of the February 2012 Cold Spell on Health in Italy Using Surveillance Data, *PLOS ONE*, 8, e61720, <https://doi.org/10.1371/journal.pone.0061720>, 2013.
- Dong, J., Peng, J., He, X., Corcoran, J., Qiu, S., and Wang, X.: Heatwave-induced human health risk assessment in megacities based on heat stress-social vulnerability-human exposure framework, *Landsc. Urban Plan.*, 203, 103907, <https://doi.org/10.1016/j.landurbplan.2020.103907>, 2020.
- 485 Dosio, A., Mentaschi, L., Fischer, E. M., and Wyser, K.: Extreme heat waves under 1.5\hspace{0.167em}°C and 2\hspace{0.167em}°C global warming, *Environ. Res. Lett.*, 13, 054006, <https://doi.org/10.1088/1748-9326/aab827>, 2018.
- 490 Dunn, P. K.: Occurrence and quantity of precipitation can be modelled simultaneously, *Int. J. Climatol.*, 24, 1231–1239, <https://doi.org/10.1002/joc.1063>, 2004.



- Dunn, P. K.: tweedie: Evaluation of Tweedie Exponential Family Models, 2021.
- Ellena, M., Ballester, J., Mercogliano, P., Ferracin, E., Barbato, G., Costa, G., and Ingole, V.: Social inequalities in heat-attributable mortality in the city of Turin, northwest of Italy: a time series analysis from 1982 to 2018, *Environ. Health*, 19, 116, <https://doi.org/10.1186/s12940-020-00667-x>, 2020.
- 495 El-Zein, A. and Tonmoy, F. N.: Assessment of vulnerability to climate change using a multi-criteria outranking approach with application to heat stress in Sydney, *Ecol. Indic.*, 48, 207–217, <https://doi.org/10.1016/j.ecolind.2014.08.012>, 2015.
- Estoque, R. C., Ooba, M., Seposo, X. T., Togawa, T., Hijioka, Y., Takahashi, K., and Nakamura, S.: Heat health risk assessment in Philippine cities using remotely sensed data and social-ecological indicators, *Nat. Commun.*, 11, 1581, <https://doi.org/10.1038/s41467-020-15218-8>, 2020.
- 500 Fratianni, S. and Acquafredda, F.: The Climate of Italy, in: *Landscapes and Landforms of Italy*, edited by: Soldati, M. and Marchetti, M., Springer International Publishing, Cham, 29–38, [https://doi.org/10.1007/978-3-319-26194-2\\_4](https://doi.org/10.1007/978-3-319-26194-2_4), 2017.
- 505 Frigerio, I. and De Amicis, M.: Mapping social vulnerability to natural hazards in Italy: A suitable tool for risk mitigation strategies, *Environ. Sci. Policy*, 63, 187–196, <https://doi.org/10.1016/j.envsci.2016.06.001>, 2016.
- García-León, D., Casanueva, A., Standardi, G., Burgstall, A., Flouris, A. D., and Nybo, L.: Current and projected regional economic impacts of heatwaves in Europe, *Nat. Commun.*, 12, 5807, <https://doi.org/10.1038/s41467-021-26050-z>, 2021.
- 510 Gasparrini, A., Guo, Y., Hashizume, M., Lavigne, E., Zanobetti, A., Schwartz, J., Tobias, A., Tong, S., Rocklöv, J., Forsberg, B., Leone, M., Sario, M. D., Bell, M. L., Guo, Y.-L. L., Wu, C., Kan, H., Yi, S.-M., Coelho, M. de S. Z. S., Saldiva, P. H. N., Honda, Y., Kim, H., and Armstrong, B.: Mortality risk attributable to high and low ambient temperature: a multicountry observational study, *The Lancet*, 386, 369–375, [https://doi.org/10.1016/S0140-6736\(14\)62114-0](https://doi.org/10.1016/S0140-6736(14)62114-0), 2015.
- 515 Goffard, P.-O., Jammalamadaka, S. R., and Meintanis, S.: Goodness-of-fit tests for compound distributions with applications in insurance, 2019.
- 520 Habeeb, D., Vargo, J., and Stone, B.: Rising heat wave trends in large US cities, *Nat. Hazards*, 76, 1651–1665, <https://doi.org/10.1007/s11069-014-1563-z>, 2015.
- Hasan, M. M. and Dunn, P. K.: Two Tweedie distributions that are near-optimal for modelling monthly rainfall in Australia, *Int. J. Climatol.*, 31, 1389–1397, <https://doi.org/10.1002/joc.2162>, 2011.
- 525 Ho, H. C., Knudby, A., Chi, G., Aminipouri, M., and Lai, D. Y.-F.: Spatiotemporal analysis of regional socio-economic vulnerability change associated with heat risks in Canada, *Appl. Geogr.*, 95, 61–70, <https://doi.org/10.1016/j.apgeog.2018.04.015>, 2018.



- Huber, P. J.: Robust Statistics, in: International Encyclopedia of Statistical Science, edited by: Lovric, M., Springer, Berlin, Heidelberg, 1248–1251, 530 [https://doi.org/10.1007/978-3-642-04898-2\\_594](https://doi.org/10.1007/978-3-642-04898-2_594), 2011.
- IPCC: Climate Change 2014 – Impacts, Adaptation and Vulnerability: Part A: Global and Sectoral Aspects: Working Group II Contribution to the IPCC Fifth Assessment Report: Volume 1: Global and Sectoral Aspects, Cambridge University Press, Cambridge, <https://doi.org/10.1017/CBO9781107415379>, 2014.
- 535 Istat.it - 15° Censimento della popolazione e delle abitazioni 2011: <https://www.istat.it/it/censimenti-permanenti/censimenti-precedenti/popolazione-e-abitazioni/popolazione-2011>, last access: 16 November 2021.
- Jarzyna, K. and Krzyżewska, A.: Cold spell variability in Europe in relation to the degree of climate continentalism in 1981–2018 period, *Weather*, 76, 122–128, 540 <https://doi.org/10.1002/wea.3937>, 2021.
- Johnson, W. D., Burton, J. H., Beyl, R. A., and Romer, J. E.: A Simple Chi-Square Statistic for Testing Homogeneity of Zero-Inflated Distributions, *Open J. Stat.*, 5, 483, <https://doi.org/10.4236/ojs.2015.56050>, 2015.
- 545 Jorgensen, B.: Exponential Dispersion Models, *J. R. Stat. Soc. Ser. B Methodol.*, 49, 127–162, 1987.
- Karanja, J. and Kiage, L.: Perspectives on spatial representation of urban heat vulnerability, *Sci. Total Environ.*, 774, 145634, <https://doi.org/10.1016/j.scitotenv.2021.145634>, 2021.
- Kendall, M. G.: Rank correlation methods, Griffin, Oxford, England, 1948.
- 550 Kim, D.-W., Deo, R. C., Lee, J.-S., and Yeom, J.-M.: Mapping heatwave vulnerability in Korea, *Nat. Hazards*, 89, 35–55, <https://doi.org/10.1007/s11069-017-2951-y>, 2017.
- King, A. D. and Harrington, L. J.: The Inequality of Climate Change From 1.5 to 2°C of Global Warming, *Geophys. Res. Lett.*, 45, 5030–5033, <https://doi.org/10.1029/2018GL078430>, 2018.
- 555 King, A. D., Donat, M. G., Lewis, S. C., Henley, B. J., Mitchell, D. M., Stott, P. A., Fischer, E. M., and Karoly, D. J.: Reduced heat exposure by limiting global warming to 1.5 °C, *Nat. Clim. Change*, 8, 549–551, <https://doi.org/10.1038/s41558-018-0191-0>, 2018.
- 560 Kishore, P., Basha, G., Venkat Ratnam, M., AghaKouchak, A., Sun, Q., Velicogna, I., and Ouarda, T. B. J. M.: Anthropogenic influence on the changing risk of heat waves over India, *Sci. Rep.*, 12, 3337, <https://doi.org/10.1038/s41598-022-07373-3>, 2022.



- Kron, W., Löw, P., and Kundzewicz, Z. W.: Changes in risk of extreme weather events in Europe, *Environ. Sci. Policy*, 100, 74–83, <https://doi.org/10.1016/j.envsci.2019.06.007>, 2019.
- 565 Liu, X., Yue, W., Yang, X., Hu, K., Zhang, W., and Huang, M.: Mapping Urban Heat Vulnerability of Extreme Heat in Hangzhou via Comparing Two Approaches, *Complexity*, 2020, e9717658, <https://doi.org/10.1155/2020/9717658>, 2020.
- López-Bueno, J. A., Navas-Martín, M. Á., Díaz, J., Mirón, I. J., Luna, M. Y., Sánchez-Martínez, G., Culqui, D., and Linares, C.: The effect of cold waves on mortality in urban and rural areas of Madrid, *Environ. Sci. Eur.*, 33, 72, <https://doi.org/10.1186/s12302-021-00512-z>, 2021.
- 570 Maragno, D., Dalla Fontana, M., and Musco, F.: Mapping Heat Stress Vulnerability and Risk Assessment at the Neighborhood Scale to Drive Urban Adaptation Planning, *Sustainability*, 12, 1056, <https://doi.org/10.3390/su12031056>, 2020.
- 575 Michelozzi, P., de 'Donato, F., Bisanti, L., Russo, A., Cadum, E., DeMaria, M., D'Ovidio, M., Costa, G., and Perucci, C. A.: Heat Waves in Italy: Cause Specific Mortality and the Role of Educational Level and Socio-Economic Conditions, in: *Extreme Weather Events and Public Health Responses*, edited by: Kirch, W., Bertollini, R., and Menne, B., Springer, Berlin, Heidelberg, 121–127, [https://doi.org/10.1007/3-540-28862-7\\_12](https://doi.org/10.1007/3-540-28862-7_12), 2005.
- 580 Michelozzi, P., De' Donato, F., Scortichini, M., De Sario, M., Asta, F., Agabiti, N., Guerra, R., de Martino, A., and Davoli, M.: [On the increase in mortality in Italy in 2015: analysis of seasonal mortality in the 32 municipalities included in the Surveillance system of daily mortality], *Epidemiol. Prev.*, 40, 22–28, <https://doi.org/10.19191/EP16.1.P022.010>, 2016.
- 585 Morabito, M., Crisci, A., Gioli, B., Gualtieri, G., Toscano, P., Stefano, V. D., Orlandini, S., and Gensini, G. F.: Urban-Hazard Risk Analysis: Mapping of Heat-Related Risks in the Elderly in Major Italian Cities, *PLOS ONE*, 10, e0127277, <https://doi.org/10.1371/journal.pone.0127277>, 2015.
- 590 Oldenborgh, G. J. van, Mitchell-Larson, E., Vecchi, G. A., Vries, H. de, Vautard, R., and Otto, F.: Cold waves are getting milder in the northern midlatitudes, *Environ. Res. Lett.*, 14, 114004, <https://doi.org/10.1088/1748-9326/ab4867>, 2019.
- Orlando, S., Mosconi, C., De Santo, C., Emberti Gialloreti, L., Inzerilli, M. C., Madaro, O., Mancinelli, S., Ciccacci, F., Marazzi, M. C., Palombi, L., and Liotta, G.: The Effectiveness of Intervening on Social Isolation to Reduce Mortality during Heat Waves in Aged Population: A Retrospective Ecological Study, *Int. J. Environ. Res. Public. Health*, 18, 11587, <https://doi.org/10.3390/ijerph182111587>, 2021.
- 595 Papathoma-Köhle, M., Ulbrich, T., Keiler, M., Pedoth, L., Totschnig, R., Glade, T., Schneiderbauer, S., and Eidswig, U.: Chapter 8 - Vulnerability to Heat Waves, Floods, and Landslides in Mountainous Terrain: Test Cases in South Tyrol, in: *Assessment of Vulnerability to Natural Hazards*, edited by: Birkmann, J., Kienberger, S., and
- 600



- Alexander, D. E., Elsevier, 179–201, <https://doi.org/10.1016/B978-0-12-410528-7.00008-4>, 2014.
- Peng, J., Liu, Y., Li, T., and Wu, J.: Regional ecosystem health response to rural land use change: A case study in Lijiang City, China, *Ecol. Indic.*, 72, 399–410, <https://doi.org/10.1016/j.ecolind.2016.08.024>, 2017.
- Perkins-Kirkpatrick, S. E. and Gibson, P. B.: Changes in regional heatwave characteristics as a function of increasing global temperature, *Sci. Rep.*, 7, 12256, <https://doi.org/10.1038/s41598-017-12520-2>, 2017.
- Perkins-Kirkpatrick, S. E. and Lewis, S. C.: Increasing trends in regional heatwaves, *Nat. Commun.*, 11, 3357, <https://doi.org/10.1038/s41467-020-16970-7>, 2020.
- Piticar, A., Croitoru, A.-E., Ciupertea, F.-A., and Harpa, G.-V.: Recent changes in heat waves and cold waves detected based on excess heat factor and excess cold factor in Romania, *Int. J. Climatol.*, 38, 1777–1793, <https://doi.org/10.1002/joc.5295>, 2018.
- Poumadère, M., Mays, C., Le Mer, S., and Blong, R.: The 2003 Heat Wave in France: Dangerous Climate Change Here and Now, *Risk Anal.*, 25, 1483–1494, <https://doi.org/10.1111/j.1539-6924.2005.00694.x>, 2005.
- Quader, M. A., Khan, A. U., and Kervyn, M.: Assessing Risks from Cyclones for Human Lives and Livelihoods in the Coastal Region of Bangladesh, *Int. J. Environ. Res. Public Health*, 14, E831, <https://doi.org/10.3390/ijerph14080831>, 2017.
- Rahma, A. and Kokonendji, C. C.: Discriminating between and within (semi)continuous classes of both Tweedie and geometric Tweedie models, *J. Stat. Comput. Simul.*, 2021.
- Reid, C. E., O'Neill Marie S., Gronlund Carina J., Brines Shannon J., Brown Daniel G., Diez-Roux Ana V., and Schwartz Joel: Mapping Community Determinants of Heat Vulnerability, *Environ. Health Perspect.*, 117, 1730–1736, <https://doi.org/10.1289/ehp.0900683>, 2009.
- Russo, S., Dosio, A., Graversen, R. G., Sillmann, J., Carrao, H., Dunbar, M. B., Singleton, A., Montagna, P., Barbola, P., and Vogt, J. V.: Magnitude of extreme heat waves in present climate and their projection in a warming world, *J. Geophys. Res. Atmospheres*, 119, 12,500–12,512, <https://doi.org/10.1002/2014JD022098>, 2014.
- Russo, S., Sillmann, J., and Fischer, E. M.: Top ten European heatwaves since 1950 and their occurrence in the coming decades, *Environ. Res. Lett.*, 10, 124003, <https://doi.org/10.1088/1748-9326/10/12/124003>, 2015.
- Russo, S., Marchese, A. F., Sillmann, J., and Immé, G.: When will unusual heat waves become normal in a warming Africa?, *Environ. Res. Lett.*, 11, 054016, <https://doi.org/10.1088/1748-9326/11/5/054016>, 2016.





- Russo, S., Sillmann, J., Sippel, S., Barcikowska, M. J., Ghisetti, C., Smid, M., and O'Neill, B.: Half a degree and rapid socioeconomic development matter for heatwave risk, *Nat. Commun.*, 10, 136, <https://doi.org/10.1038/s41467-018-08070-4>, 2019.
- 640 Schiavina, M., Freire, S., and MacManus, K.: GHS-POP R2019A - GHS population grid multitemporal (1975-1990-2000-2015), <https://doi.org/10.2905/0C6B9751-A71F-4062-830B-43C9F432370F>, 2019.
- 645 Serrano-Notivol, R., Lemus-Canovas, M., Barrao, S., Sarricolea, P., Meseguer-Ruiz, O., and Tejedor, E.: Heat and cold waves in mainland Spain: Origins, characteristics, and trends, *Weather Clim. Extrem.*, 37, 100471, <https://doi.org/10.1016/j.wace.2022.100471>, 2022.
- Smid, M., Russo, S., Costa, A. C., Granell, C., and Pebesma, E.: Ranking European capitals by exposure to heat waves and cold waves, *Urban Clim.*, 27, 388–402, <https://doi.org/10.1016/j.uclim.2018.12.010>, 2019.
- 650 Spinoni, J., Lakatos, M., Szentimrey, T., Bihari, Z., Szalai, S., Vogt, J., and Antofie, T.: Heat and cold waves trends in the Carpathian Region from 1961 to 2010, *Int. J. Climatol.*, 35, 4197–4209, <https://doi.org/10.1002/joc.4279>, 2015.
- 655 Taleghani, M., Marshall, A., Fitton, R., and Swan, W.: Renaturing a microclimate: The impact of greening a neighbourhood on indoor thermal comfort during a heatwave in Manchester, UK, *Sol. Energy*, 182, 245–255, <https://doi.org/10.1016/j.solener.2019.02.062>, 2019.
- Tijdeman, E., Stahl, K., and Tallaksen, L. M.: Drought Characteristics Derived Based on the Standardized Streamflow Index: A Large Sample Comparison for Parametric and Nonparametric Methods, *Water Resour. Res.*, 56, <https://doi.org/10.1029/2019WR026315>, 2020.
- 660 Tuholske, C., Caylor, K., Funk, C., Verdin, A., Sweeney, S., Grace, K., Peterson, P., and Evans, T.: Global urban population exposure to extreme heat, *Proc. Natl. Acad. Sci.*, 118, e2024792118, <https://doi.org/10.1073/pnas.2024792118>, 2021.
- 665 Tweedie, M. C. K.: An index which distinguishes between some important exponential families, in: *Statistics: applications and new directions* (Calcutta, 1981), *Indian Statist. Inst.*, Calcutta, 579–604, 1984.
- Disaster risk: <https://www.undrr.org/terminology/disaster-risk>, last access: 21 November 2021.
- 670 Vu, A., Rutherford, S., and Phung, D.: Heat Health Prevention Measures and Adaptation in Older Populations—A Systematic Review, *Int. J. Environ. Res. Public Health*, 16, 4370, <https://doi.org/10.3390/ijerph16224370>, 2019.
- Watts, N., Amann, M., Arnell, N., Ayeb-Karlsson, S., Belesova, K., Berry, H., Bouley, T., Boykoff, M., Byass, P., Cai, W., Campbell-Lendrum, D., Chambers, J., Daly, M.,





- 675 Dasandi, N., Davies, M., Depoux, A., Dominguez-Salas, P., Drummond, P., Ebi, K. L.,  
 Ekins, P., Montoya, L. F., Fischer, H., Georgeson, L., Grace, D., Graham, H., Hamilton,  
 I., Hartinger, S., Hess, J., Kelman, I., Kiesewetter, G., Kjellstrom, T., Kniveton, D.,  
 Lemke, B., Liang, L., Lott, M., Lowe, R., Sewe, M. O., Martinez-Urtaza, J., Maslin, M.,  
 McAllister, L., Mikhaylov, S. J., Milner, J., Moradi-Lakeh, M., Morrissey, K., Murray, K.,  
 Nilsson, M., Neville, T., Oreszczyn, T., Owfi, F., Pearman, O., Pencheon, D., Pye, S.,  
 680 Rabbaniha, M., Robinson, E., Rocklöv, J., Saxer, O., Schütte, S., Semenza, J. C.,  
 Shumake-Guillemot, J., Steinbach, R., Tabatabaei, M., Tomei, J., Trinanes, J., Wheeler,  
 N., Wilkinson, P., Gong, P., Montgomery, H., and Costello, A.: The 2018 report of the  
 Lancet Countdown on health and climate change: shaping the health of nations for  
 centuries to come, *The Lancet*, 392, 2479–2514, [https://doi.org/10.1016/S0140-6736\(18\)32594-7](https://doi.org/10.1016/S0140-6736(18)32594-7), 2018.
- 685 Zhang, R., Sun, C., Zhu, J., Zhang, R., and Li, W.: Increased European heat waves in  
 recent decades in response to shrinking Arctic sea ice and Eurasian snow cover, *Npj  
 Clim. Atmospheric Sci.*, 3, 1–9, <https://doi.org/10.1038/s41612-020-0110-8>, 2020.